Carbohydrate Research 457 (2018) 32–40

Contents lists available at ScienceDirect

Carbohydrate Research

journal homepage: www.elsevier.com/locate/carres

Synthesis of sulfamide analogues of deoxythymidine monophosphate as potential inhibitors of mycobacterial cell wall biosynthesis

Kajitha Suthagar [a], Wanting Jiao [a, e], Hélène Munier-Lehmann [b, c], Antony J. Fairbanks [a, d, *]

[a] Department of Chemistry, University of Canterbury, Private Bag 4800, Christchurch, 8140, New Zealand
[b] Institut Pasteur, Unité de Chimie et Biocatalyse, 28 rue du Dr Roux, 75724, Paris Cedex 15, France
[c] CNRS UMR3523, 28 rue du Dr Roux, France
[d] Biomolecular Interaction Centre, University of Canterbury, Private Bag 4800, Christchurch, 8140, New Zealand
[e] Ferrier Research Institute, Victoria University of Wellington, PO Box 600, Wellington, 6140, New Zealand

ARTICLE INFO

Article history:
Received 21 November 2017
Received in revised form
8 January 2018
Accepted 8 January 2018
Available online 11 January 2018

Keywords:
Carbohydrates
Sulfamides
Deoxythymidine
Mycobacteria
Tuberculosis
Thymidine monophosphate kinase

ABSTRACT

The recently discovered enzyme *Mycobacterium tuberculosis* thymidine monophosphate kinase (TMPK*mt*), which catalyses the phosphorylation of deoxythymidine monophosphate (dTMP) to give deoxythymidine diphosphate (dTDP), is indispensable for the growth and survival of *M. tuberculosis* as it plays an essential role in DNA synthesis. Inhibition of TMPK*mt* is an attractive avenue for the development of novel anti-tuberculosis agents. Based on the premise that sulfamide may be a suitable isostere of phosphate, deoxythymidine analogues comprising various substituted sulfamides at C5′ were modelled *in silico* into the active site of TMPK*mt* (PDB accession code: 1N5K) using induced-fit docking methods. A selection of modelled compounds was synthesized, and their activity as inhibitors of TMPK*mt* was evaluated. Three compounds showed competitive inhibition of TMPK*mt* in the micromolar range (10 −50 μM). Compounds were tested *in vitro* for anti-mycobacterial activity against *M. smegmatis*: three compounds showed weak anti-mycobacterial activity (MIC 250 μg/mL).

1. Introduction

Tuberculosis (TB) is one of the primary infectious diseases worldwide, especially in developing countries. *Mycobacterium tuberculosis* is recognised as the causative agent of TB [1]. TB has affected humans since antiquity, and remains as a major threat to human health. Alarmingly up to one third of the world's population is currently latently infected, and 10.4 million new cases and 1.4 million deaths were reported in 2016 [2]. People infected by Human Immunodeficiency Virus (HIV) are at an especially high risk of contracting TB due to their compromised immune system. In many countries, the rate of increase of infection is exacerbated by both poor public health and apparent synergism with HIV [2,3]. The resurgence of the disease has prompted interest in increasing understanding of TB and the development of new anti-mycobacterial agents against drug-resistant tuberculosis.

The current requirement for long duration treatments and the emergence of multi- (MDR-TB) and extensively drug resistant (XDR-TB) forms of *M. tuberculosis* represent significant challenges in the effective treatment of tuberculosis [4]. The discovery of new mycobacterial targets and the development of agents that require shorter treatment durations are essential to combat the rise of MDR-TB and XDR-TB.

The recently discovered enzyme *Mycobacterium tuberculosis* thymidine monophosphate kinase (TMPK*mt*) is indispensable for the growth and survival of *M. tuberculosis*, as it plays an essential role in DNA synthesis [5]. TMPK*mt* catalyses the phosphorylation of deoxythymidine monophosphate (dTMP **1a**) to give deoxythymidine diphosphate (dTDP **1b**) using ATP as the phosphoryl donor (Fig. 1), and is essential for maintaining the deoxythymidine triphosphate pool that is required for DNA synthesis and bacterial replication. This phosphorylation step occurs at the junction of the *de novo* and salvage pathways in the biosynthesis of deoxythymidine triphosphate (dTTP). Importantly TMPK*mt* has low (22%) sequence identity with the human isozyme, and therefore represents a promising target for the development of selective inhibitors [6].

The synthesis of potential inhibitors of TMPK*mt* has previously been reported by Van Calenbergh [7–10] and several others

* Corresponding author. Department of Chemistry, University of Canterbury, Private Bag 4800, Christchurch, 8140, New Zealand.
E-mail address: antony.fairbanks@canterbury.ac.nz (A.J. Fairbanks).

https://doi.org/10.1016/j.carres.2018.01.001
0008-6215/

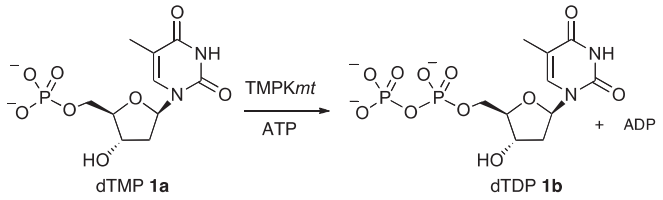

Fig. 1. Action of TMPK*mt*.

[11–15], including a series of 5′-thiourea-substitued α-thymidine derivatives [10] which displayed promising inhibitory activity; these had K_is vs. TMPK*mt* in the 0.17–260 μM range, and also inhibited *M. bovis* in Alamar Blue assays with minimum inhibitory concentrations (MICs) in the range from 20 to 100 μg/mL [7,10].

Although the synthesis and biological activities of various sulfonamides and sulfamates have been widely reported, there are only a limited number of investigations into sulfamides as possible phosphate isosteres. Amongst these limited studies, Aldrich [16,17] reported the use of sulfamide as an isosteric replacement for phosphate in the search for anti-mycobacterial agents by way of their inhibition of siderophore biosynthesis; in this case salicyl sulfamoyl adenosine and its derivatives displayed promising inhibitory activity, with MICs ranging from 0.19 to 6.25 μg/mL against *M. tuberculosis*.

Previously we reported the synthesis and biological activity [18] of a series of *arabino*-glycosyl sulfamides as potential mimics of decaprenolphosphoarabinose (DPA), and thus as novel anti-mycobacterial agents. Crystallographic studies performed during that work showing the clear tetrahedral geometry at sulphur gave further credence to the idea that this interesting and under-explored motif may have value in the design of new pharmacological agents comprising sulfamide as a phosphate isostere. In line with our on-going interest in the development of new anti-mycobacterial agents, the design and synthesis of sulfamides as analogues of deoxythymidine monophosphate was selected as an avenue for study. We report herein the *in silico* modelling of a variety of sulfamide analogues of dTMP **1a** into the active site of TMPK*mt* using induced-fit docking methods [19], the synthesis of a selection of these compounds and their evaluation *in vitro* as inhibitors of TMPK*mt*, and finally a study of their anti-mycobacterial activity against *M. smegmatis*.

2. Results and discussion

2.1. Docking studies

A small library of sulfamide analogues of dTMP **1a** was designed and screened with the published three-dimensional structure of TMPK*mt* (PDB accession code: 1N5K) [20], using an induced fit docking method with Schrödinger Suite 2014 [21,22]. Firstly the natural substrate dTMP was modelled back into the active site (Fig. 2) with a rigid docking protocol in Glide [23], and it was confirmed that the binding mode of the substrate could be successfully reproduced by docking calculations [20].

Next, in order to investigate the binding affinity of a variety of sulfamide structures, a number of target compounds was selected (Fig. 3). Besides simple alkylated (**2a-c, 2f**) and un-substituted (**2g**) sulfamides a variety of other compounds comprising substituted aromatic rings was also selected in order to study any importance of aryl substituents. In particular since Van Calenbergh had previously shown that a variety of thiourea derivatives of thymidine [8,10] possessing 3-trifluoromethyl-4-chloro- and halogenated phenyl rings had displayed promising inhibitory activity (with K_is

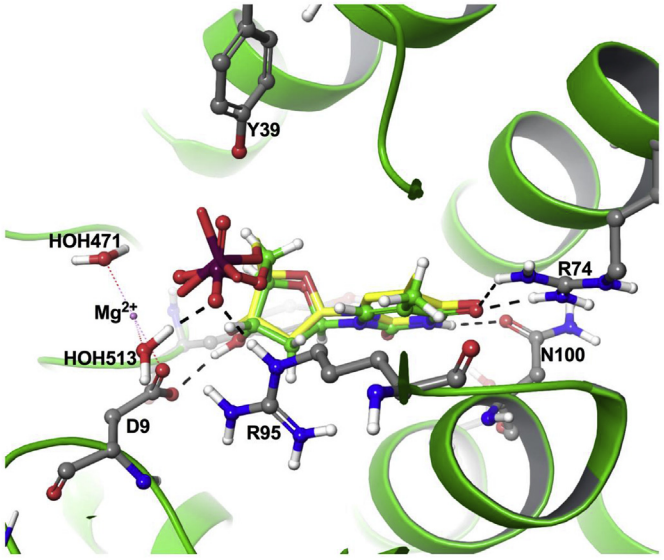

Fig. 2. Superimposition of the modelled dTMP **1a** conformation (green carbon atoms) with that found in the reported crystal structure (yellow carbon atoms) in the active site of TMPK*mt* (PDB: 1N5K, displayed with grey carbon atoms and green ribbon). Hydrogen bonds formed between the modelled conformation of dTMP and the active site are shown as black dashed lines. (For interpretation of the references to colour in this figure legend, the reader is referred to the Web version of this article.)

vs. TMPK*mt* in the 0.17–3.2 μM range), a variety of sulfamides containing these structural motifs was selected. Additionally since these studies had also highlighted the potential for α-thymidine derivatives to inhibit TMPK*mt*, the corresponding α-anomers **2p-r** were also considered. Compounds **2a-r** were then modelled into the TMPK*mt* active site using the induced fit docking protocol [22], and the docking scores are listed in Table 1.

Non-substituted sulfamide **2g** is the structurally most similar analogue to dTMP, and gave a docking score of −12.153 kcal/mol, suggesting that the binding affinity of compound **2g** should actually be less than that of the natural substrate dTMP **1a** (−14.611 kcal/mol). As shown in Fig. 4, the sulfamide group of sulfamide **2g** is located in close proximity to the phosphate-binding site. The phosphate group of the natural substrate dTMP **1a** forms H-bonds with a water molecule and Arg95 (R95: Fig. 2). In the case of the sulfamide **2g**, there is no strong interaction with Arg95 due to the lack of a full negative charge on the sulfamide. However the N-H groups of the sulfamide **2g** are seen to form H-bonds with the OH group of Tyr39 (Y39: Fig. 4), providing an example of an additional interaction that may increase compound binding affinity.

The docking scores of the compounds screened ranged from −10.9 to −12.6 kcal/mol. In fact surprisingly all sulfamides, except the trifluoroethyl substituted sulfamide **2f**, gave docking scores which were similar to sulfamide **2g**, i.e. in the range from −11 to −12 kcal/mol, suggesting that adding extra functional groups to the sulfamide may not improve binding. Furthermore the binding poses predicted by the induced-fit docking suggested that additional groups would be mostly solvent exposed, as there is not sufficient space in the active site to accommodate extra groups. However, in a few cases the docking studies predicted extra binding interactions between amino acids of the protein and additional functional groups incorporated into the substituted sulfamides. For example, docking of azidophenyl substituted sulfamide **2k** predicted the formation of a pi-cation interaction between Arg95 (R95) and the aromatic ring, and a salt bridge between Asp94 (D94) and the azide (Fig. 5A). Furthermore, docking of the trifluoromethyl substituted phenyl sulfamide **2h** also revealed a pi-cation interaction between the substituted aromatic

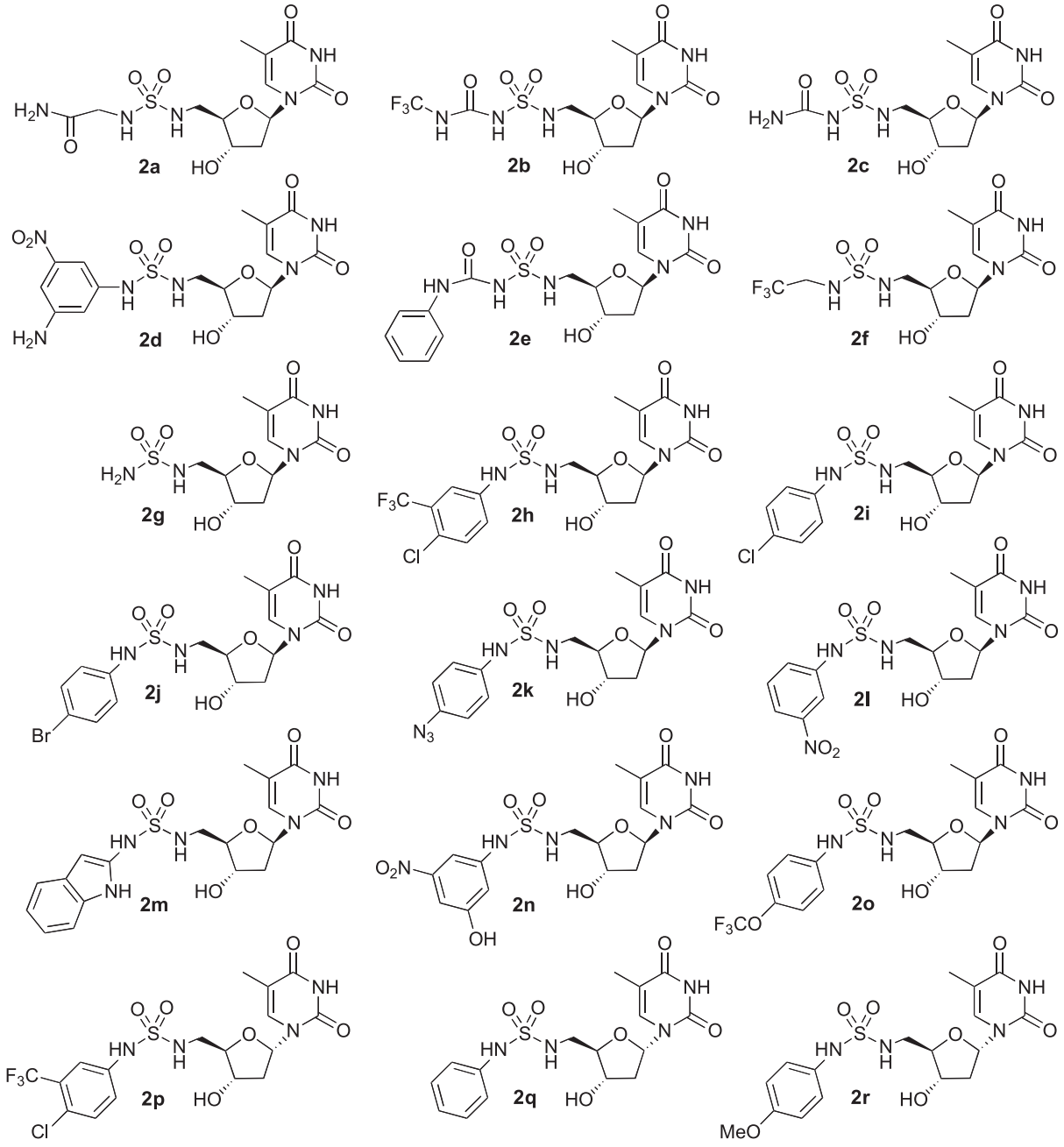

Fig. 3. Sulfamide structures selected as potential analogues of dTMP **1a** for docking into the active site of TMPK*mt*.

ring and Arg153 (R153) (Fig. 5B).

2.2. Synthesis

Since all compounds (except **2f**) had displayed similar docking scores, a small number were selected as synthetic targets; if interesting inhibitory activity were observed the remainder would then be synthesised at a later point in time. In line with the reports [8,10] that thiourea derivatives of thymidine comprised of 3-trifluoromethyl-4-chloro- and halogenated phenyl rings had promising inhibitory activity vs. TMPK*mt* (*vide supra*), compounds **2h-j** were initially selected for synthesis. Additionally for comparison the non-substituted sulfamide **2g**, and also the azide **2k**, which was predicted to have an extra binding interaction as outlined above, were also selected as synthetic targets.

A simple strategy to access an analogue of dTMP **1a** which comprises a sulfamide at position 6′ involves reaction of 6′-amino-2′-deoxythymidine **11** with a suitable sulfamoyl chloride. In these cases the required sulfamoyl chlorides were accessed from the corresponding aniline derivatives, which were themselves synthesized as shown in Scheme 1. Nitration of commercially available 2-chlorobenzotrifluoride **3** was carried out using a 1:1 mixture of concentrated HNO_3 and H_2SO_4 to afford **4** [24], which was then reduced by catalytic hydrogenation in the presence of 10% Pd on carbon in MeOH under an atmosphere of hydrogen to yield aniline derivative **5a**. Alternatively the aryl azide **5d** was synthesized from commercially available 4-bromoaniline **6**, using a proline-promoted CuI-catalysed Ullmann-type coupling [25]. The

Table 1
Results of docking sulfamides into the active site of TMPK*mt*.

Compound	Glide gscore[a] (kcal/mol)	IFD score[b] (kcal/mol)
dTMP **1a**	−14.611	–
2a	−11.856	−9398.257
2b	−12.233	−9387.295
2c	−12.375	−9380.878
2d	−11.982	−9376.289
2e	−11.526	−9371.215
2f	−10.981	−9370.213
2g	−12.153	−9357.980
2h	−11.594	−9350.776
2i	−12.341	−9365.354
2j	−12.074	−9349.660
2k	−11.846	−9366.776
2l	−11.784	−9354.936
2m	−11.560	−9354.338
2n	−11.922	−9348.174
2o	−11.771	−9347.914
2p	−11.331	−9346.145
2q	−12.649	−9345.166
2r	−11.189	−9329.090

[a] Glide gscore = Empirical scoring function that approximates the ligand binding free energy.
[b] IFD score = Induced fid docking score; IFD score = 1.0*Prime energy + 9.057*Glide score + 1.428*Glide Ecoul.

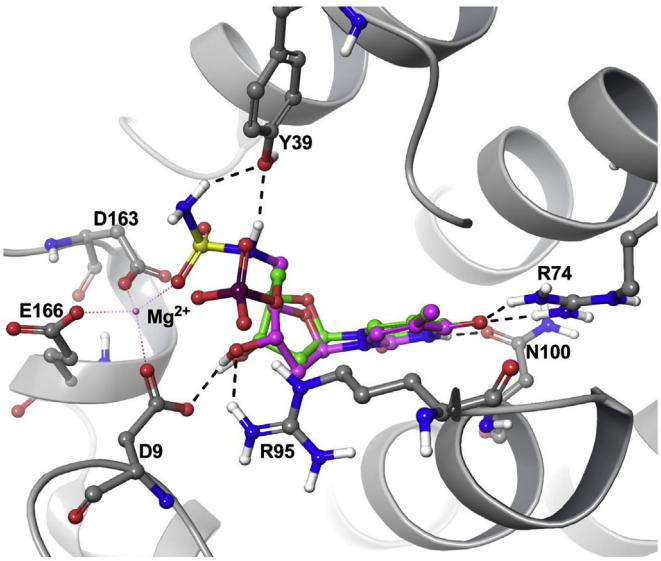

Fig. 4. Superimposition of the predicted binding conformation of compound **2g** (obtained from induced-fit docking, magenta carbon atoms) with that of the substrate dTMP **1a** (green carbon atoms) in the active site of TMPK*mt*. Hydrogen bonds formed between compound **2g** and the active site residues are displayed as black dashed lines, whilst interactions formed between dTMP **1a** and the active site are not displayed for reasons of clarity. (For interpretation of the references to colour in this figure legend, the reader is referred to the Web version of this article.)

required sulfamoyl chlorides **7a-d** were then synthesized using **5a**, **5d** and additionally the commercially available amines **5b** and **5c**, by conversion into the corresponding *N*-sulfonic acid, and then chlorination using PCl_5 (Scheme 1).

The required coupling partner 6′-amino-2′-deoxythymidine **11** was accessed from deoxythymidine **8** (Scheme 2). Firstly iodide **9** was produced *via* selective iodination of the primary alcohol of **8** by treatment with PPh_3, I_2, and imidazole [26], and then converted to azide **10** by treatment with NaN_3. Catalytic hydrogenation in the presence of 10% Pd on carbon in MeOH then gave the desired amine **11**. Reaction of amine **11** with either NH_2SO_2Cl or sulfamoyl chlorides **7a-d** in the presence of Et_3N finally gave the desired sulfamides **2g-k** respectively.

2.3. Biological assays

Firstly sulfamides **2g-k** were evaluated for TMPKmt inhibition as described in Section 3.3; the results are summarized in Table 2. Compounds **2g,h,j** were found to be competitive inhibitors of TMPKmt, with Ki values in the micromolar range. Competitive inhibition was demonstrated by performing the assays at two different concentrations of dTMP (0.5 and 0.05 mM). Sulfamide **2h** was the most potent with Ki value of 12 μM. On the other hand, compounds **2j** and **2g** were found to inhibit TMPKmt although with lower potency (~2- and ~4-fold decreases, respectively) than compound **2h**. Unfortunately the assays did not provide conclusive results for the inhibitory potency of compounds **2i** and **2k**, the latter case probably due to issues of compound solubility.

Sulfamides **2g-k** were then tested for anti-mycobacterial activity against *M. smegmatis* using an Alamar Blue assay as described in Section 3.4 [27]. Ethambutol (**EB**, MIC 0.5 μg/mL) was also assayed as a control. The results are shown in Fig. 6 and Table 3.

As can be seen from Table 3 none of the compounds displayed significant inhibitory activity against *M. smegmatis*. The unsubstituted sulfamide **2g** did not inhibit growth of *M. smegmatis* at concentrations up to 1000 μg/mL. Although this may possibly be due to the hydrophilic nature of the sulfamide moiety in **2g** (cLogP: −1.68), which may limit membrane permeability, it should be noted that Aldrich and co-workers [17] have produced significantly more active compounds (e.g. MIC vs. *M. tuberculosis* of 0.39 μg/mL) of similar polarity (e.g. cLogP: −0.89).

Aryl substituted sulfamides **2h-2j**, all of which contain a halogenated phenyl ring as the sulfamide substituent, did display low anti-mycobacterial activity, with MICs of 250 μg/mL, although the activity did not depend on the identity of the halogen substituent. Interestingly the presence of an azide on the phenyl ring in compound **2k** led to a greater than 4-fold loss in activity against *M. smegmatis* (MIC > 1000 μg/mL).

Some comments on the results of the *in silico* docking studies, the measured inhibitory activities against TMPK*mt*, and the *in vitro* assays against *M. smegmatis* are necessary. The docking studies indicated that broadly similar binding affinities to TMPK*mt* were expected for the synthesized compounds. The enzymatic assays against to TMPK*mt* showed that compound **2h** was the most potent inhibitor of TMPK*mt* (in the micromolar range), and was slightly stronger than compounds **2j** and **2g** (by a factor of ~2 and ~4 respectively). No reliable values could be obtained for the other two compounds (**2i,k**). Unfortunately because of safety and regulatory issues, it was necessary to use *M. smegmatis* rather than *M. tuberculosis* for the anti-mycobacterial assays. Conclusions as to the lack of significant *in vitro* anti-mycobacterial activity are therefore harder to delineate, but given the low activities (micromolar) observed v.s. TMPK*mt* the benefit of establishing an assay v.s. *M. tuberculosis* is not clear. In terms of correlating the *in silico* and anti-mycobacterial assays, a better approach would have been to dock the sulfamides into an X-ray structure of the corresponding enzyme (TMPK*ms*) from *M. smegmatis*; however no such structure is available.

3. Conclusion

A variety of sulfamide analogues of dTMP **1a** were designed and docked into the active site of the *M. tuberculosis* enzyme TMPK*mt*. Except for sulfamide **2f**, all the compounds studied *in silico* gave similar docking scores, which ranged from −11 to −12 kcal/mol. Five of these compounds **2g-k** were then synthesised and their activity as inhibitors of TMPK*mt* was measured. Three compounds

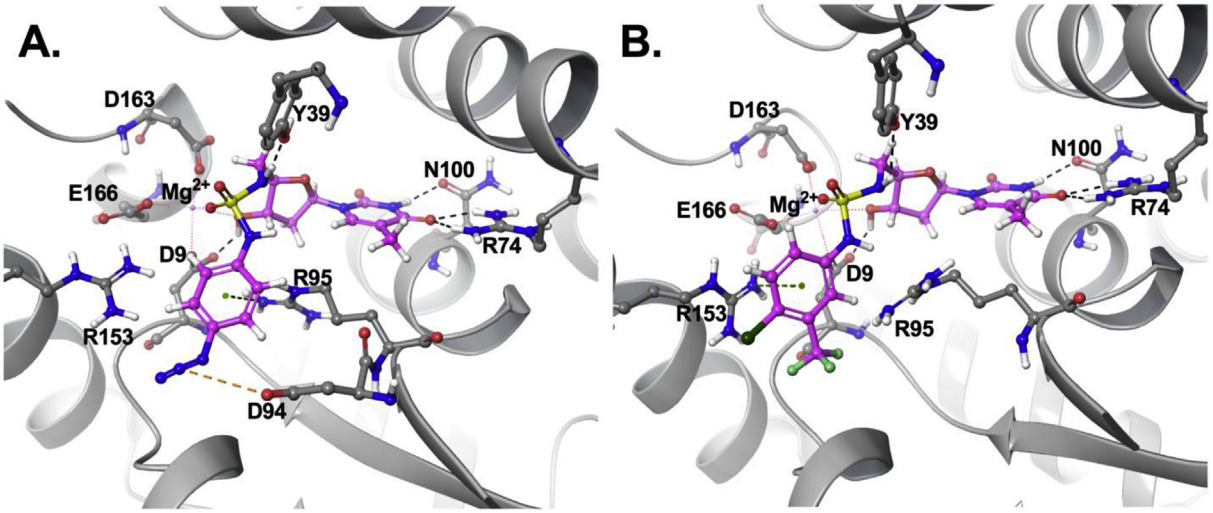

Fig. 5. Predicted binding poses of (**A**) compound **2k** (magenta carbon atoms) and (**B**) compound **2h** (magenta carbon atoms) in the active site of TMPK*mt*. Hydrogen bonding interactions are displayed as black dashed lines, pi-cation interactions are displayed as green dashed lines, and salt-bridge interactions are displayed as orange dashed lines. (For interpretation of the references to colour in this figure legend, the reader is referred to the Web version of this article.)

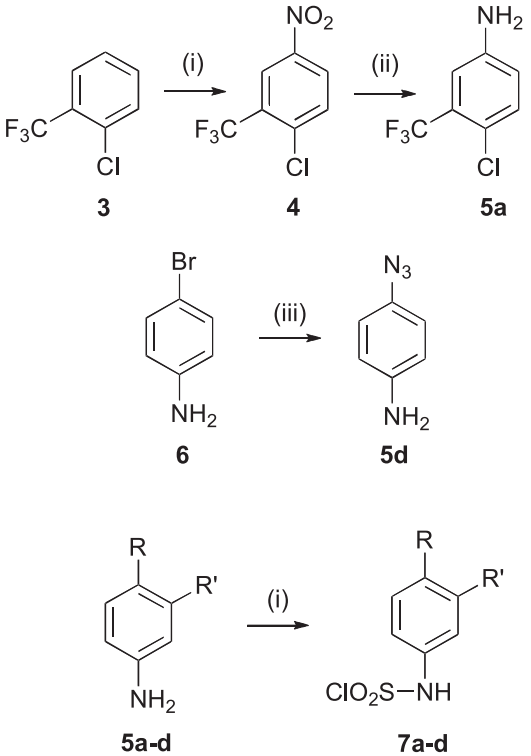

Scheme 1. (i) HNO_3, H_2SO_4, 50–60 °C, 1 h, 72%; (ii) Pd/C, H_2, MeOH, rt, 2 h, 69%; (iii) NaN_3, CuI, proline, NaOH, EtOH, H_2O, 75 °C, 3 h, 48%; (iv) HSO_3Cl, Et_3N, DCM, −9 °C to rt, 1 h; then PCl_5, toluene, 80 °C, 2 h.

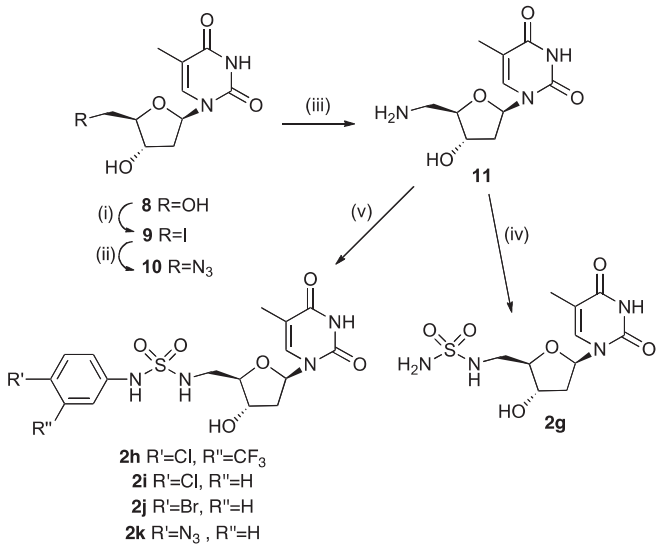

Scheme 2. (i) PPh_3, I_2, imidazole, THF, 60 °C, 16 h, 41%; (ii) NaN_3, DMF, 50 °C, 16 h, 70%; (iii) PPh_3, H_2O, rt, 16 h, 60%; (iv) NH_2SO_2Cl, Et_3N, DMA, 0 °C to rt, 2 h, 74%; (v) Et_3N, **7a-d**, CH_3CN, 0 °C to rt, 2 h; **2h**, 65%; **2i**, 49%; **2j**, 41%; **2k**, 34%.

were found to be competitive inhibitors, with Ki values in the micromolar range. Assays of compounds **2g-k** *in vitro* against *M. smegmatis* revealed that aryl sulfamides **2h-j** with halogen substituents did inhibit mycobacterial growth, with MICs of 250 μg/mL. However, none of these compounds showed inhibitory activity that was promising enough to merit further investigation.

4. Experimental

4.1. Molecular docking procedure

The three-dimensional crystal structure of TMPK*mt* in complex with dTMP substrate was imported from the PDB (accession code: 1N5K) [20]. TMPK*mt* is a homodimer and each monomer has 214 amino acids [28]. The receptor structure was prepared in the semi-closed state, which is more representative of the active site conformation when substrate is bound. Protein preparation wizard (one of the most frequently used tools and techniques in structure preparation) [29] was used to add hydrogens, assign bond orders, create

Table 2
Inhibitory potency of sulfamide analogues of dTMP **2g-k** on TMPKmt enzymatic activity.

Compound	Ki (μM)
2g	50 ± 5
2h	12 ± 3
2i	ND
2j	27 ± 7
2k	ND[a]

ND, not determined.
[a] Interference with the assay due to solubility issues.

Table 3
Anti-mycobacterial activity of sulfamide analogues of dTMP **2g-k** vs. *M. smegmatis*.

Compound	MIC (μg/mL)[a]
Ethambutol (**EB**)	0.5
2g	>1000
2h	250
2i	250
2j	250
2k	>1000

[a] MIC = minimum inhibitory concentration; the lowest concentration of the compound which inhibited the growth of *M. smegmatis* >90% in the Alamar Blue assay. Ethambutol (EB, MIC 0.5 μg/mL) was used as a control.

zero-order bonds to metals, and fill in missing side chains. For rigid docking of the substrate back to the active site, the two water molecules that coordinate to the metal ion were kept in the structure; all other water molecules were removed. The receptor structure was refined by sampling water orientations and assigning protonation states using PROPKA [30]. Then the structure was minimized with a convergence of heavy atoms set to a root-mean-square deviation (RMSD) of 0.30 Å, which is measure of average atomic distance between the atoms. The receptor grid for rigid docking of substrate was generated in Glide using co-crystallized ligand (dTMP) to define the centre of the grid box [29]. All other settings were kept as default.

The target compounds including the substrate molecule were built in Maestro [21], and prepared using LigPrep [31]. The substrate was docked into the receptor grid file using Glide with the XP (extra precision) mode [32].

For target compounds, an induced fit docking protocol was employed. For induced fit docking, the two water molecules that were coordinated to the active site metal ion were removed. The centre of the grid was defined as the centroid of the bound substrate in the original crystal structure. After the initial docking stage, all active site residues within a 5 Å distance of the docked ligands were refined to optimize interactions with the docked ligand. The ligands were then re-docked to the refined receptor conformation using XP mode. The predicted binding poses for each compound were then examined.

4.2. Synthesis

4.2.1. General

Melting points were recorded on an Electrothermal® melting point apparatus. Proton and carbon nuclear magnetic resonance (δ_H, δ_C) spectra were recorded on Bruker AV 400 (400 MHz), or Bruker AV 500 (500 MHz) spectrometers. All chemical shifts are quoted on the δ-scale in ppm using residual solvent as an internal standard. High-resolution mass spectra were recorded on a Bruker FT-ICR electrospray ionisation mass spectrometer, using either electrospray ionisation techniques as stated. *M/z* values are reported in Daltons and are followed by their percentage abundance in parentheses. Optical rotations were measured on a Perkin-Elmer 241 polarimeter with a path length of 1 dm. Concentrations are given in g/100 mL. Thin Layer Chromatography (t.l.c.) was carried out on Merck Silica gel $60F_{254}$ aluminium-backed plates. Visualisation of the plates was achieved using a u.v. lamp ($\lambda_{max} = 254$ or 365 nm), and/or ammonium molybdate (5% in 2 M sulphuric acid), or sulphuric acid (5% in ethanol). Flash column chromatography was carried out using Sorbsil C60 40/60 silica. Reverse phase high performance liquid chromatography (RP-HPLC) was performed on a Dionex P680 HPLC instrument with a Phenomenex Luna C 18 (2) 100 A column (5 μm, 10 × 250 mm) at 40 °C. The column was eluted with a gradient of MeCN/H_2O at a flow rate of 1 mL min^{-1}. Alcohol-free dichloromethane was dried on an alumina column. Anhydrous DMF, pyridine, methanol and toluene were purchased from Sigma Aldrich. 'Petrol' refers to the fraction of light petrol ether boiling in the range of 40–60 °C.

4.2.2. General procedure A

Amine **11** (1 equiv.) was dissolved in dry acetonitrile and the mixture stirred at 0 °C under nitrogen (5 mL). Triethylamine (3 equiv.) and sulfamoyl chloride (2 equiv.) were then added, the reaction was then allowed to warm to room temperature, and stirred for 2 h. Then the solvent was removed *in vacuo* to give a residue that was then purified by RP-HPLC (Luna C-18 column (Phenomenex);

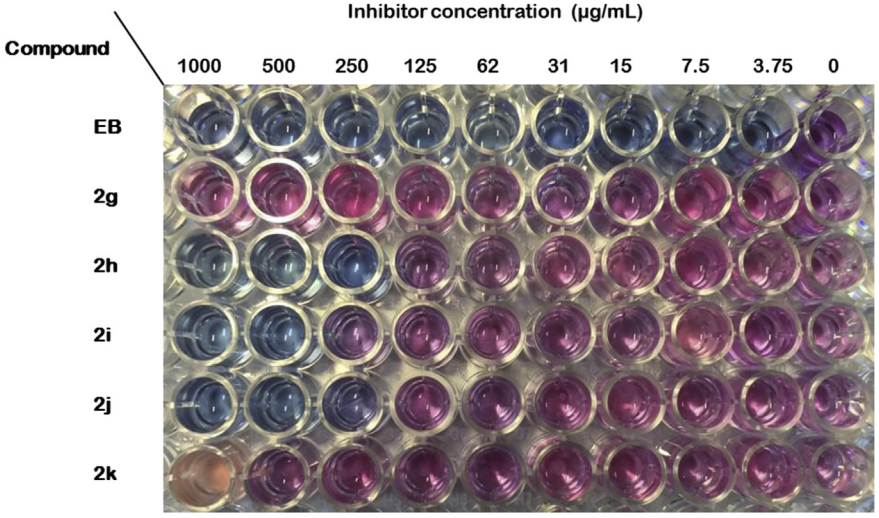

Fig. 6. Alamar Blue assay of sulfamides **2g-k** vs *M. smegmatis* plus control.

eluent: A (0.05% TFA in H_2O) and B MeCN; gradient: the sample was run at 1 mL/min with a gradient 0–45% B; column oven: 40 °C; detection: UV 210 nm and 280 nm) to afford sulfamide.

4.2.3. General procedure for the synthesis of sulfamoyl chlorides **7a-d**

Triethylamine (9 equiv.) was added to a solution of aniline **5a-d** (1 equiv.) in $CHCl_3$ (20 mL). Chlorosulfonic acid (1 equiv.) was added dropwise at −9 °C (ice and salt water mixture). The solution was then stirred at −2 °C for 1 h before it was concentrated *in vacuo.* The crude residue was dissolved in NaOH (1N, 20 mL) and then the resulting mixture was concentrated *in vacuo*. The residue was suspended in boiling ethanol. The insoluble solids were filtered off, and the filtrate was concentrated *in vacuo* to afford *N*-phenylsulfamate. The crude residue *N*-Phenylsulfamate was co-evaporated with toluene (3 × 30 mL) and then the residue was dissolved in toluene. PCl_5 (1 equiv.) was added and the reaction mixture was refluxed for 2 h, and then cooled to room temperature. The resulting suspension was filtered, and the filtrate was concentrated *in vacuo* to afford sulfamoyl chloride **7a-d**, which was used in the next step without further purification.

4.2.4. 2-Chloro-5-nitrobenzotrifluoride 4 [24]

Conc. HNO_3 (2.7 mL, 0.06 mol) was added drop-wise to conc. H_2SO_4 (3.1 mL, 0.06 mol). The resulting mixture was cooled to 20 °C and then 2-chlorobenzotrifluoride **3** (1 g, 5.5 mmol) was added. The reaction was stirred for 1 h at 50 °C until gas evolution ceased. After this time, t.l.c. (Petrol) indicated the formation of a single product (R_f 0.1). Iced water (50 mL) was then added carefully. The solvent was then removed *in vacuo* to give a residue that was then purified by flash chromatography to afford nitro compound **4** (0.9 g, 72%) as pale yellow oil. δ_H (400 MHz, $CDCl_3$) 7.72 (1H, d, *J* 9.0 Hz, Ar-H-3), 8.35 (1H, dd, *J* 8.6, 2.7 Hz, Ar-H-4), 8.58 (1H, d, *J* 2.4 Hz, Ar-H-6).

4.2.5. 5-Amino-2-chlorobenzotrifluoride ***5a*** [24]

10% Activated Pd-C (118 mg) was added to a solution of nitro compound **4** (1 g, 4.5 mmol) in methanol (20 mL). The flask was evacuated and purged with nitrogen five times, before being placed under an atmosphere of hydrogen. The solution was stirred for 2 h at room temperature. After this time, t.l.c. (petrol: EtOAc 4:1) indicated the formation of a product (R_f 0.5), and complete consumption of starting material (R_f 0.8). The reaction mixture was filtered through Celite® (eluting with methanol, 20 mL), and concentrated *in vacuo* to give a residue which was purified by flash column chromatography to afford aniline **5a** (1.2 g, 68.9%) as yellow oil. δ_H (400 MHz, $CDCl_3$) 6.72 (1H, dd, *J* 8.4 Hz, 2.5 Hz, Ar-H-6), 6.95 (1H, d, *J* 2.7 Hz, Ar-H-5), 7.22 (1H, d, *J* 8.6 Hz, Ar-H-2).

4.2.6. 4-Azidoaniline ***5d*** [25]

Sodium ascorbate (345 mg, 1.7 mmol, 0.3 equiv.), CuI (330 mg, 1.7 mmol, 0.3 equiv.), L-proline (200 mg, 1.7 mmol, 0.3 equiv.) and NaOH (70 mg, 1.7 mmol, 0.3 equiv.) were added to a solution of 4-bromoaniline **6** (1 g, 5.8 mmol, 1 equiv.) in EtOH: H_2O (7:3, 30 mL). The resulting mixture was stirred for 15 min at room temperature. Then sodium azide (755 mg, 11.6 mmol, 2 equiv.) was added and the reaction mixture was stirred at reflux for 3 h. After this time, t.l.c (DCM 100%) indicated the formation of a single product (R_f 0.35), and complete consumption of starting material (R_f 0.4). The reaction mixture was cooled and concentrated *in vacuo.* The residue was dissolved in EtOAc (50 mL) and washed with water (3 × 50 mL). The combined organic extracts were dried over anhydrous $MgSO_4$, filtered, and concentrated in *vacuo*, which was then purified by flash chromatography (DCM 100%) to afford aniline **5d** (373 mg, 48%) as brown solid. m.p 62–63 °C (DCM) [lit 65–66 °C] [25,33]; δ_H (400 MHz, CD_3OD) [33] 6.60 (2H, d, *J* 8.6 Hz, Ar-H), 7.15 (2H, d, *J* 8.6 Hz, Ar-H).

4.2.7. 5′-Deoxy-5′-iodo-β-D-thymidine 9 [34]

Thymidine **8** (1.0 g, 4.1 mmol, 1 equiv.) was dissolved in dry THF (25 mL) and triphenylphosphine (2.16 g, 8.2 mmol, 2 equiv.), iodine (1.57 g, 6.1 mmol 1.5 equiv.) and imidazole (421 mg, 6.1 mmol, 1.5 equiv.) were then added sequentially. The reaction mixture was then heated to 50 °C and stirred at for 16 h under nitrogen. After this time, t.l.c. (DCM: MeOH, 19:1) indicated the formation of a single product (R_f 0.2). The mixture was cooled, the solvent was removed *in vacuo*, and the residue was then dissolved in DCM (30 mL). The resulting solution was washed with 1 M aqueous HCl (20 mL). The organic extracts were dried over anhydrous $MgSO_4$, filtered, and concentrated *in vacuo* to give a residue that was then purified by flash chromatography (gradient elution, 100% DCM to DCM: MeOH, 97:3) to afford iodide **9** (0.6 g, 41%) as a white solid. m.p 168–170 °C (DCM/Petrol) [lit 170–173 °C] [34]; $[\alpha]_D$ [20] +22.8 (*c*, 1.0 in CH_3OH); δ_H (500 MHz, CD_3OD) 1.90 (3H, d, *J* 1.3 Hz, 5-CH_3), 2.26–2.34 (2H, m, H-2a', H-2b'), 3.43–3.53 (2H, m, H-5a', H-5b'), 3.83–3.86 (1H, m, H-4′), 4.29–4.32 (1H, m, H-3′), 6.28 (1H, t, $J_{1,2}$ 7.0 Hz, H-1′), 7.61 (1H, d, *J* 1.3 Hz, H-6).

4.2.8. 5′-Azido-5′-deoxy-β-D-thymidine 10 [35]

Iodide **9** (0.6 g, 1.7 mmol, 1 equiv.) was dissolved in dry DMF (10 mL), and NaN_3 (336 mg, 5.2 mmol, 3 equiv.) was then added. The reaction mixture was heated to 50 °C and stirred for 16 h under nitrogen. After this time, t.l.c. (EtOAc) indicated the formation of a single product (R_f 0.1), and the complete consumption of starting material (R_f 0.2). The mixture was cooled, the solvent was removed *in vacuo*, and the residue was dissolved in ethyl acetate (30 mL). The solution was washed with water (3 × 20 mL) and brine (20 mL). The organic extracts were dried over anhydrous $MgSO_4$, filtered, and concentrated *in vacuo* to give a residue that was then purified by flash chromatography (EtOAc 100%) to afford 5′-azido-2′,5′-dideoxy-β-D-thymidine **10** (0.27 g, 70%) as a white solid. m.p 157–159 °C (EtOH/Et_2O) [lit 161–163 °C] [36]; $[\alpha]_D$ [20] +66.4 (*c*, 0.5 in CH_3OH) [lit. $[\alpha]_D$ [22] +89.5 (*c*, 0.94 in CH_3OH)] [37]; δ_H (500 MHz, CD_3OD) 1.89 (3H, d, *J* 1.1 Hz, 5-CH_3), 2.24–2.31 (2H, m, H-2a', H-2b'), 3.50–3.64 (2H, m, H-5a', H-5b'), 3.96 (1H, aq, *J* 3.9 Hz, H-4′), 4.33–4.37 (1H, m, H-3′), 6.26 (1H, t, $J_{1,2}$ 6.8 Hz, H-1′), 7.54 (1H, d, *J* 1.3 Hz, H-6).

4.2.9. 5′-Amino-5′-deoxy-β-D-thymidine 11 [33]

Azide **10** (130 mg, 0.5 mmol, 1 equiv.) was dissolved in dry THF (10 mL). Triphenylphosphine (255 mg, 1.0 mmol, 2 equiv.) and water (0.02 mL, 1.0 mmol, 2 equiv.) were then added. The reaction mixture was stirred at room temperature for 16 h under nitrogen. After this time, t.l.c. (DCM: MeOH, 19:1) indicated the formation of a single product (R_f 0.0), and the complete consumption of starting material (R_f 0.6). The solvent was removed *in vacuo* to give a residue that was then purified by flash chromatography (2%–10% MeOH/DCM) to afford amine **11** (70 mg, 60%) as a white solid. m.p 165–167 °C (EtOH/Et_2O) [lit 173.5–174.5 °C] [33]; $[\alpha]_D$ [20] +11.6 (*c*, 0.5 in CH_3OH) [lit. $[\alpha]_D$ [26] +39 (*c*, 1.0 in CH_3OH)] [33]; δ_H (400 MHz, CD_3OD) 1.75 (3H, s, 5-CH_3), 2.16–2.34 (2H, m, H-2a', H-2b'), 2.74–2.93 (2H, m, H-5a', H-5b'), 3.80–3.86 (1H, m, H-4′), 4.22–4.29 (1H, m, H-3′), 6.12 (1H, t, $J_{1,2}$ 6.8 Hz, H-1′), 7.30 (1H, s, H-6).

4.2.10. 5′-Deoxy-5′-[N-(sulfamoyl)amino]-β-D-thymidine ***2g***

General Procedure A, using sulfamoyl chloride, and purification by RP-HPLC (Luna C-18 column (Phenomenex); eluent: A (0.05% TFA in H_2O) and B MeCN; gradient: the sample was run at 1 mL/min with a gradient of 0–45% B; column oven: 40 °C; detection: UV 210 nm and 280 nm), afforded sulfamide **2g** (68 mg, 74%) as a pale

yellow waxy solid. $[\alpha]_D$ [20] +14.3 (*c*, 0.35 in CH_3OH); υ_{max} (neat) 3268 (N-H), 1350 (s, S=O), 1170 (s, S=O) cm^{-1}; δ_H (400 MHz, D_2O) 1.76 (3H, s, 5-CH_3), 2.55–2.75 (2H, m, H-2a', H-2b'), 3.17–3.40 (2H, m, H-5a' and H-5b'), 4.28–4.36 (1H, m, H-4′), 5.03–5.12 (1H, m, H-3′), 6.01 (1H, t, $J_{1,2}$ 7.0 Hz, H-1′), 7.34 (1H, s, H-6); δ_C (100 MHz, D_2O) 11.3 (q, 5-CH_3), 35.2 (t, C-2′), 40.6 (t, C-5′), 79.7 (d, C-3′), 79.8 (d, C-4′), 88.0 (d, C-1′), 111.2 (s, C-5), 139.4 (d, C-6), 151.4 (s, C-2), 166.5 (s, C-4); HRMS (ESI) calculated for $C_{10}H_{17}N_4O_6S$: 321.0863. Found 321.0873 (MH^+).

4.2.11. 5′-Deoxy-5′-N-[N-(3-trifluoromethyl-4-chlorophenyl) sulfamoyl]amino]-β-D-thymidine **2h**

General Procedure A, using sulfamoyl chloride **7a,** and purification by RP-HPLC (Luna C-18 column (Phenomenex); eluent: A (0.05% TFA in H_2O) and B MeCN; gradient: the sample was run at 1 mL/min with a gradient of 0–45% B; column oven: 40 °C; detection: UV 210 nm and 280 nm), afforded sulfamide **2h** (43 mg, 65%) as a pale yellow solid. m.p 105–107 °C (EtOH/Et_2O); $[\alpha]_D$ [20] +10.3 (*c*, 0.35 in CH_3OH); υ_{max} (neat) 3273 (N-H), 1370 (s, S=O), 1165 (s, S=O) cm^{-1}; δ_H (500 MHz, CD_3OD) 1.86 (3H, d, *J* 1.0 Hz, 5-CH_3), 2.18–2.23 (2H, m, H-2a', H-2b'), 3.19 (1H, dd, $J_{5a',5b'}$ 14.6 Hz, $J_{4,5a'}$6.6 Hz, H-5a'), 3.28 (1H, dd, $J_{5a',5b'}$ 13.6 Hz, $J_{4,5b'}$ 4.5 Hz, H-5b'), 3.85–3.87 (1 H, m, H-4′), 4.25–4.27 (1 H, m, H-3′), 6.11 (1H, t, $J_{1,2}$ 6.8 Hz, H-1′), 7.41 (1H, dd, *J* 8.9 Hz, 2.7 Hz, Ar-H-6), 7.47 (1H, d, *J* 1.0 Hz, H-6), 7.49 (1H, d, *J* 8.9 Hz, Ar-H-5), 7.57 (1H, d, *J* 2.7 Hz, Ar-H-2); δ_C (100 MHz, CD_3OD) 10.9 (q, 5-CH_3), 38.7 (t, C-2′), 44.2 (t, C-5′), 71.2 (d, C-3′), 84.6 (d, C-4′), 85.5 (d, C-1′), 110.3 (s, C-5), 117.3, 122.7, 131.9 (d, q, Ar(C)H, CF_3), 136.9 (d, C-6), 137.0, 138.0 (2 × s, 3 x Ar(C)), 150.8 (s, C-2), 164.9 (s, C-4); HRMS (ESI) calculated for $C_{17}H_{19}ClF_3N_4O_6S$: 499.0660. Found 499.0677 (MH^+).

4.2.12. 5′-N-[N-(4-Chlorophenyl)sulfamoyl]amino]- 5′-deoxy-β-D-thymidine **2i**

General Procedure A, using sulfamoyl chloride **7b,** and purification by RP-HPLC (Luna C-18 column (Phenomenex); eluent: A (0.05% TFA in H_2O) and B MeCN; gradient: the sample was run at 1 mL/min with a gradient of 0–45% B; column oven: 40 °C; detection: UV 210 nm and 280 nm), afforded sulfamide **2i** (26 mg, 49%) as a white solid. m.p 105–107 °C (EtOH/Et_2O); $[\alpha]_D$ [20] +22.4 (*c*, 0.25 in CH_3OH); υ_{max} (neat) 3207 (N-H), 1328 (s, S=O), 1150 (s, S=O) cm^{-1}; δ_H (400 MHz, CD_3OD) 1.87 (3H, s, 5-CH_3), 2.20 (2H, at, *J* 6.3 Hz, H-2a', H-2b'), 3.13–3.28 (2H, m, H-5a' and H-5b'), 3.85(1 H, aq, *J* 4.7 Hz, H-4′), 4.28 (1 H, aq, *J* 5.1 Hz, H-3′), 6.12 (1H, t, $J_{1,2}$ 7.0 Hz, H-1′), 7.18, 7.26(4H, 2 × d, *J* 8.2 Hz, 4 × Ar-H), 7.50 (1H, s, H-6); δ_C (100 MHz, CD_3OD) 10.9 (q, 5-CH_3), 38.8 (t, C-2′), 44.2 (t, C-5′), 71.2 (d, C-3′), 84.7 (d, C-4′), 85.5 (d, C-1′), 110.3 (s, C-5), 120.3, 128.6 (2 × d, 4 × Ar(C)H), 137.0 (d, C-6), 137.2 (s, 2 × Ar(C)), 150.8 (s, C-2), 165.0 (s, C-4); HRMS (ESI) calculated for $C_{16}H_{20}ClN_4O_6S$: 431.0787. Found 431.0788 (MH^+).

4.2.13. 5′-N-[N-(4-Bromophenyl)sulfamoyl]amino]- 5′-deoxy-β-D-thymidine **2j**

General Procedure A, using sulfamoyl chloride **7c,** and purification by RP-HPLC (Luna C-18 column (Phenomenex); eluent: A (0.05% TFA in H_2O) and B MeCN; gradient: the sample was run at 1 mL/min with a gradient of 0–45% B; column oven: 40 °C; detection: UV 210 nm and 280 nm), afforded sulfamide **2j** (24 mg, 41%) as a white solid. m.p 115–117 °C (EtOH/Et_2O); $[\alpha]_D$ [20] +15.2 (*c*, 0.25 in CH_3OH); υ_{max} (neat) 3208 (N-H), 1386 (s, S=O), 1150 (s, S=O) cm^{-1} δ_H (400 MHz, CD_3OD) 1.87 (3H, s, 5-CH_3), 2.18 (2H, at, *J* 6.3 Hz, H-2a', H-2b'), 3.14–3.28 (2H, m, H-5a' and H-5b'), 3.85 (1 H, aq, *J* 5.1 Hz, H-4′), 4.27 (1 H, aq, *J* 4.7 Hz, H-3′), 6.11 (1H, t, $J_{1,2}$ 7.0 Hz, H-1′), 7.13 (2H, d, *J* 8.6 Hz, 2 × Ar-H), 7.40 (2H, d, *J* 9.0 Hz, 2 × Ar-H), 7.50 (1H, s, H-6); δ_C (100 MHz, CD_3OD) 11.0 (q, 5-CH_3), 38.8 (t, C-2′), 44.2 (t, C-5′), 71.2 (d, C-3′), 84.7 (d, C-4′), 85.5 (d, C-1′), 110.3 (s, C-5), 120.5, 131.7 (2 × d, 4 × Ar(C)H), 137.0 (d, C-6), 137.7 (s, 2 × Ar(C)), 150.8 (s, C-2), 165.0 (s, C-4); HRMS (ESI) calculated for $C_{16}H^{79}_{20}BrN_4O_6S$: 431.0281. Found 475.0281 (MH^+).

4.2.14. 5′-N-[N-(4-Azidophenyl)sulfamoyl]amino]- 5′-deoxy-β-D-thymidine **2k**

General Procedure A, using sulfamoyl chloride **7d,** and purification by RP-HPLC (Luna C-18 column (Phenomenex); eluent: A (0.05% TFA in H_2O) and B MeCN; gradient: the sample was run at 1 mL/min with a gradient of 0–45% B; column oven: 40 °C; detection: UV 210 nm and 280 nm), afforded sulfamide **2k** (18 mg, 34%) as a light brown solid. m.p 133–135 °C (EtOH/Et_2O); $[\alpha]_D$ [20] +10.4 (*c*, 0.25 in CH_3OH); υ_{max} (neat) 3219 (N-H), 1331 (s, S=O), 1148 (s, S=O) cm^{-1}; δ_H (400 MHz, CD_3OD) 1.86 (3H, s, 5-CH_3), 2.19 (2H, at, *J* 6.3 Hz, H-2a', H-2b'), 3.13–3.28 (2H, m, H-5a' and H-5b'), 3.86 (1 H, aq, *J* 4.7 Hz, H-4′), 4.27 (1 H, aq, *J* 5.1 Hz, H-3′), 6.11 (1H, t, $J_{1,2}$ 7.0 Hz, H-1′), 6.98, 7.23 (4H, 2 × d, *J* 8.6 Hz, 4 × Ar-H), 7.49 (1H, s, H-6); δ_C (100 MHz, CD_3OD) 10.9 (q, 5-CH_3), 38.8 (t, C-2′), 44.2 (t, C-5′), 71.1 (d, C-3′), 84.7 (d, C-4′), 85.5 (d, C-1′), 110.3 (s, C-5), 119.2, 121.0 (2 × d, 4 × Ar(C)H), 137.0 (d, C-6), 137.2 (s, 2 × Ar(C)), 150.8 (s, C-2), 165.0 (s, C-4); HRMS (ESI) calculated for $C_{16}H_{20}N_7O_6S$: 438.1190. Found 438.1200 (MH^+).

4.3. Measurement of TMPKmt enzymatic activity

The reaction medium (0.5 mL final volume) contained 50 mM Tris-HCl pH 7.4, 50 mM KCl, 2 mM $MgCl_2$, 0.2 mM NADH, 1 mM phosphoenol pyruvate and 2 units each of lactate dehydrogenase, pyruvate kinase and nucleoside diphosphate kinase. Activity was determined using the coupled spectrophotometric assay at 334 nm (0.5 mL final) in an Eppendorf ECOM 6122 photometer [38]. One unit of enzyme activity corresponds to 1 μmole of the product formed in 1 min at 30 °C and pH 7.4. The concentration of ATP (0.5 mM) and dTMP (0.05 or 0.5 mM) was kept constant, whereas the concentrations of the sulfamide analogues were varied between 0.06 and 0.6 mM.

4.4. Measurement of anti-mycobacterial activity vs. M. smegmatis

The anti-mycobacterial activities of sulfamides **2g-k** were performed using *M. smegmatis*. Test compounds and ethambutol (EB) were prepared in DMSO at 40 mg/mL, and subsequent 2 fold serial dilutions were performed in 100 μl of LB/T media and DMSO (1.25%) in 96 well microplates, producing compound concentrations across the plate of 1000, 500, 250, 125, 62, 31, 15, 7.5, and 3.75 μg/mL. Following the serial dilation each well had a constant concentration of DMSO (2.5%). Approximately 4.5×10^6 cfu/mL of *M. smegmatis* was added to each well, to give a total volume of 200 μl. Control wells contained only bacteria with 2.5% DMSO in LB/T media. The plates were incubated at 37 °C for 18 h. After this time, 10 μl of Alamar Blue dye was added to all wells, and the plate was then incubated for a further 5 h. The wells were then observed for a colour change (blue to pink), and the MIC value was determined visually.

Acknowledgements

The authors thank the University of Canterbury (PhD Scholarship to KS) and the Biomolecular Interaction Centre for financial support. Hélène Munier-Lehmann was supported by INSERM, CNRS and the Institut Pasteur.

References

[1] T.M. Daniel, Respir. Med. 100 (2006) 1862–1870.
[2] WHO, Global Tuberculosis Report, 2015, pp. 1–115. http://www.who.int/tb/

en/.
[3] A. Koul, E. Arnoult, N. Lounis, J. Guillemont, K. Andries, Nature 469 (2011) 483–490.
[4] G.S. Besra, P.J. Brennan, J. Pharm. Pharmacol. 49 (1997) 25–30.
[5] C.H. Andrade, K.F. Pasqualoto, E.I. Ferreira, A.J. Hopfinger, J. Chem. Inf. Med. 49 (2009) 1070–1078.
[6] H. Munier-Lehmann, A. Chaffotte, S. Pochet, G. Labesse, Protein Sci. 10 (2001), 1195–12059.
[7] S. Van Calenbergh, S. Pochet, H. Munier-Lehmann, Curr. Top. Med. Chem. 12 (2012) 694–705.
[8] S. Van Poecke, H. Munier-Lehmann, O. Helynck, M. Froeyen, S. Van Calenbergh, Bioorg. Med. Chem. 19 (2011) 7603–7611.
[9] K.S. Toti, F. Verbeke, M.D. Risseeuw, V. Frecer, H. Munier-Lehmann, S. Van Calenbergh, Bioorg. Med. Chem. 21 (2013) 257–268.
[10] I. Van Daele, H. Munier-Lehmann, M. Froeyen, J. Balzarini, S. Van Calenbergh, J. Med. Chem. 50 (2007) 5281–5292.
[11] P. Van Rompaey, K. Nauwelaerts, V. Vanheusden, J. Rozenski, H. Munier-Lehmann, P. Herdewijn, S. Van Calenbergh, Eur. J. Org. Chem. 2003 (2003) 2911–2918.
[12] L.A. Alexandrova, V.O. Chekhov, E.R. Shmalenyuk, S.N. Kochetkov, R.A. El-Asrar, P. Herdewijn, Bioorg. Med. Chem. 23 (2015) 7131–7137.
[13] A. Adamska, A. Rumijowska-Galewicz, A. Ruszczynska, M. Studzinska, A. Jablonska, E. Paradowska, E. Bulska, H. Munier-Lehmann, J. Dziadek, Z.J. Lesnikowski, A.B. Olejniczak, Eur. J. Med. Chem. 121 (2016) 71–81.
[14] O. Familiar, H. Munier-Lehmann, J.A. Ainsa, M.J. Camarasa, M.J. Perez-Perez, Eur. J. Med. Chem. 45 (2010) 5910–5918.
[15] C. Gasse, D. Douguet, V. Huteau, G. Marchal, H. Munier-Lehmann, S. Pochet, Bioorg. Med. Chem. 16 (2008) 6075–6085.
[16] R.V. Somu, H. Boshoff, C. Qiao, E.M. Bennett, C.E. Barry, C.C. Aldrich, J. Med. Chem. 49 (2005) 31–34.
[17] K.M. Nelson, K. Viswanathan, S. Dawadi, B.P. Duckworth, H.I. Boshoff, C.E. Barry, C.C. Aldrich, J. Med. Chem. 58 (2015) 5459–5475.
[18] K. Suthagar, M.I.J. Polson, A.J. Fairbanks, Org. Biomol. Chem. 13 (2015) 6573–6579.
[19] R.A. Friesner, J.L. Banks, R.B. Murphy, T.A. Halgren, J.J. Klicic, D.T. Mainz, M.P. Repasky, E.H. Knoll, M. Shelley, J.K. Perry, J. Med. Chem. 47 (2004) 1739–1749.
[20] E. Fioravanti, A. Haouz, T. Ursby, H. Munier-Lehmann, M. Delarue, D. Bourgeois, J. Mol. Biol. 327 (2003) 1077–1092.
[21] Schrodinger LLC Maestro, Schrodinger, LLC, NewYork, 2014.
[22] L.L.C. Schrodinger, Schrodinger Suite Induced Fit Protocol, Prime, Schrodinger, LLC, NewYork, 2014.
[23] Schrodinger LLC Glide, Schrodinger, LLC, NewYork, 2014.
[24] M.R. Yazdanbakhsh, N.O. Mahmoodi, S. Dabiry, Mendeleev Commun. 16 (2006) 192–194.
[25] W. Zhu, D. Ma, Chem. Commun. 7 (2004) 888–889.
[26] S.K.V. Vernekar, L. Qiu, J. Zacharias, R.J. Geraghty, Z. Wang, Med. Chem. Commun. 5 (2014) 603–608.
[27] L.A. Collins, S.G. Franzblau, Antimicrob. Agents Chemother. 41 (1997) 1004–1009.
[28] V. Frecer, P. Seneci, S. Miertus, J. Comput. Aided Mol. Des. 25 (2011) 31–49.
[29] G.M. Sastry, M. Adzhigirey, T. Day, R. Annabhimoju, W. Sherman, J. Comput. Aided Mol. Des 27 (2013) 221–234.
[30] M. Rostkowski, M.H. Olsson, C.R. Søndergaard, J.H. Jensen, BMC Struct. Biol. 11 (2011) 1.
[31] Schrodinger LLC LigPrep, Schrodinger, LLC, NewYork, 2014.
[32] R.A. Friesner, R.B. Murphy, M.P. Repasky, L.L. Frye, J.R. Greenwood, T.A. Halgren, P.C. Sanschagrin, D.T. Mainz, J. Med. Chem. 49 (2006) 6177–6196.
[33] M. Zeng, Y.H. Yang, J.J. Li, Y. Chen, D.M. Cui, C. Zhang, Asian J. Chem. 27 (2015) 1698.
[34] R. Liboska, J. Snasel, I. Barvik, M. Budesinsky, R. Pohl, Z. Tocik, O. Pav, D. Rejman, P. Novak, I. Rosenberg, Org. Biomol. Chem. 9 (2011) 8261–8267.
[35] J.P. Horwitz, A.J. Tomson, J.A. Urbanski, J. Chua, J. Org. Chem. 27 (1962) 3045–3048.
[36] J. Hiebl, E. Zbiral, J. Balzarini, E. De Clercq, J. Med. Chem. 34 (1991) 1426–1430.
[37] K. Schwekendiek, H. Kobarg, L. Daumlechner, F.D. Sonnichsen, T.K. Lindhorst, Chem. Commun. 47 (2011) 9399–9401.
[38] C. Blondin, L. Serina, L. Wiesmüller, A.-M. Gilles, O. Bârzu, Anal. Biochem. 220 (1994) 219–221.